Journal of Materials Science: Materials in Medicine

Dry versus hydrated collagen scaffolds: are dry states representative of hydrated states?

--Manuscript Draft--

Manuscript Number:	
Full Title:	Dry versus hydrated collagen scaffolds: are dry states representative of hydrated states?
Article Type:	Original Research
Corresponding Author:	Tomas Suchy, Ph.D. Institute of Rock Structure and Mechanics, Czech Academy of Science Prague, CZECH REPUBLIC
Corresponding Author Secondary Information:	
Corresponding Author's Institution:	Institute of Rock Structure and Mechanics, Czech Academy of Science
Corresponding Author's Secondary Institution:	
First Author:	Tomas Suchy, Ph.D.
First Author Secondary Information:	
Order of Authors:	Tomas Suchy, Ph.D.
	Monika Šupová
	Martin Bartoš
	Radek Sedláček
	Marco Piola
	Monica Soncini
	Gianfranco Beniamino Fiore
	Pavla Sauerová
	Marie Hubálek Kalbáčová
Order of Authors Secondary Information:	
Funding Information:	Ministerstvo Zdravotnictví Ceské Republiky (15-25813A) — Dr. Marie Hubálek Kalbáčová
	Research and Development for Innovations Operational Programme (CZ.1.05/41.00/16.0346) — Dr. Marie Hubálek Kalbáčová
	Ministry of Education, Youth and Sports of the Czech Republic (Progres Q29/1LF) — Dr. Marie Hubálek Kalbáčová
	GAUK (400215) — Dr. Pavla Sauerová
	RVO (67985891) — Dr. Tomas Suchy
Abstract:	Collagen composite scaffolds have been used for a number of studies in tissue engineering. The hydration of such highly-porous and hydrophilic structures may influence mechanical behaviour and porosity due to swelling. The differences in physical properties following hydration would represent a significant limiting factor for the seeding, growth and differentiation of cells in vitro and the overall applicability of such hydrophilic materials in vivo. Scaffolds based on collagen matrix, poly(DL-lactide) nanofibers, calcium phosphate particles and sodium hyaluronate with 8 different material compositions were characterized in the dry and hydrated states using X-ray micro-computed tomography, compression tests, hydraulic permeability measurement,

	degradation tests and infrared spectrometry. Hydration, simulating the conditions of cell seeding and cultivation up to 48 hours and 576 hours, was found to exert a minor effect on the morphological parameters and permeability. Conversely, hydration had a major statistically significant effect on the mechanical behaviour of all the tested scaffolds. The elastic modulus and compressive strength of all the scaffolds decreased by approx. 95%. The quantitative results provided confirm the importance of analysing scaffolds in the hydrated rather than the dry state since the former more precisely simulates the real environment for which such materials are designed.
Suggested Reviewers:	Michelle Ngiam National University of Singapore, Centre for Life Sciences, Singapore michelle.ngiam@nus.edu.sg
	Ryan K. Roeder Department of Aerospace and Mechanical Engineering, Bioengineering Graduate Program, University of Notre Dame, Notre Dame, IN, USA rroeder@nd.edu
	Guoping Chen Tissue Regeneration Materials Unit, International Center for Materials Nanoarchitectonics, National Institute for Materials Science, Tsukuba, Japan guoping.chen@nims.go.jp

Dry versus hydrated collagen scaffolds: are dry states representative of hydrated states?

Tomáš Suchý[1,2], Monika Šupová[1], Martin Bartoš[3], Radek Sedláček[2], Marco Piola[4], Monica Soncini[4], Gianfranco Beniamino Fiore[4], Pavla Sauerová[5,6], Marie Hubálek Kalbáčová[5,6]

[1] Department of Composites and Carbon Materials, Institute of Rock Structure and Mechanics, Academy of Sciences of the Czech Republic, V Holesovickach 41, Prague 8, 182 09, Czech Republic

[2] Laboratory of Biomechanics, Department of Mechanics, Biomechanics and Mechatronics, Faculty of Mechanical Engineering, Czech Technical University in Prague, Technicka 4, Prague 6, 166 07, Czech Republic

[3] Department of Stomatology, First Faculty of Medicine, Charles University and General University Hospital in Prague, Katerinska 32, 12801, Prague 2, Czech Republic

[4] Dipartimento di Elettronica, Informazione e Bioingegneria, Politecnico di Milano, Piazza Leonardo da Vinci 32, 20133 Milano, Italy

[5] Biomedical Centre, Faculty of Medicine in Pilsen, Charles University, Alej Svobody 76, Pilsen, Czech Republic

[6] Institute of Inherited Metabolic Disorders, 1st Faculty of Medicine, Charles University in Prague, Ke Karlovu 2, Prague 2, 128 08, Czech Republic

Corresponding author: Tomáš Suchý, suchyt@irsm.cas.cz, +420 777 608 280

Abstract

Collagen composite scaffolds have been used for a number of studies in tissue engineering. The hydration of such highly-porous and hydrophilic structures may influence mechanical behaviour and porosity due to swelling. The differences in physical properties following hydration would represent a significant limiting factor for the seeding, growth and differentiation of cells *in vitro* and the overall

applicability of such hydrophilic materials *in vivo*. Scaffolds based on collagen matrix, poly(DL-lactide) nanofibers, calcium phosphate particles and sodium hyaluronate with 8 different material compositions were characterized in the dry and hydrated states using X-ray micro-computed tomography, compression tests, hydraulic permeability measurement, degradation tests and infrared spectrometry. Hydration, simulating the conditions of cell seeding and cultivation up to 48 hours and 576 hours, was found to exert a minor effect on the morphological parameters and permeability. Conversely, hydration had a major statistically significant effect on the mechanical behaviour of all the tested scaffolds. The elastic modulus and compressive strength of all the scaffolds decreased by approx. 95%. The quantitative results provided confirm the importance of analysing scaffolds in the hydrated rather than the dry state since the former more precisely simulates the real environment for which such materials are designed.

Keywords

collagen scaffolds; hydrated states; micro-CT; scaffold swelling; mechanical properties

1. Introduction

Bone tissue engineering represents an appealing approach to the treatment of bone defects arising from bone damage associated with a range of diseases, trauma, inflammation, tumour surgery and non-union bone repair following fracturing. Bone substitutes, generated via a tissue engineering approach, allow the functioning of repair mechanisms by providing a temporary porous scaffold that, in turn, provides mechanical support for cells up to the time that the tissue has regenerated and remodelled itself naturally. These scaffolds can be seeded with specific cells and coated with signalling molecules in order to maximise both tissue growth and the rate of degradation. Optimal bone replacement materials imitate real bone composition and structure. Such composite materials combine the advantages of synthetic and natural biodegradable polymers such as collagen, and bioactive inorganic components. However, collagen-based scaffolds exhibit relatively poor mechanical

properties. Cell-seeded collagen scaffolds can be improved through *in vitro* matrix production and mineralisation. Jungreuthmayer et al. [1] employed numerical simulations to demonstrate that relatively low values of fluid velocity and wall shear stress are sufficient to initiate the *in vitro* bone formation process in cell-seeded collagen-based scaffolds with a mean pore size of 96 μm.

Other crucial features of scaffolds for bone tissue engineering are the topological characteristics of the 3D structure: scaffold porosity, pore size, interconnectivity and tortuosity. From a fluidic point of view, the effect of all these parameters can be summarized in the scaffold permeability, which could be tailored by tuning properly the scaffold topology. In the case of collagen--based composite, the pore size and porosity features could be controlled in final collagen concentration [2] and freezing rate [3] foregoing the lyophilisation process. In addition, hydraulic permeability affects nutrient/oxygen diffusion and waste removal of cells within the scaffold and, more importantly, plays a crucial role in promoting or inhibiting cell proliferation and differentiation, and cell migration eventually conditioning the tissue regeneration process.

Collagen- and gelatine-based scaffolds have been characterised in various ways in both the dry and wet (hydrated) states; naturally they are always hydrated *in vivo*. It is known that both collagen and gelatine as well as other natural polymers such as chitosan are hydrophilic as a result of their polar groups and, thus, scaffolds are subject to swelling [4]. A larger swelling index may be ascribed to higher porosity and greater average pore size, which facilitate the penetration of water into the scaffolds [5]. Significant differences in swelling index can also be ascribed to various degrees of crosslinking [6]. A greater collagen concentration in the precursor slurry causes an increase in both pore wall closure and the thickness of the pore walls which, together, lead to greater volume swelling on hydration. Conversely, the penetration of water into a scaffold may cause the swelling of the hydrophilic parts of the scaffold and, consequently, a decrease in porosity in the hydrated state [7] and, in some cases, even the closure of the pores [8]. Increasing pore wall closure has been found to determine the time-

dependent nature of the hydrated scaffold response, with a decrease in permeability [9]. Varley et al. [10] determined (by comparing scaffolds in the dry and hydrated states) that hydration caused an increase in pore structure diameter (approx. 20%), while connectivity decreased by around 40%.

The hydrated state can also strongly affect the mechanical properties of scaffolds [11]. It is known that the Young's modulus of 3D scaffolds depends upon the relative density of the sponge, the elastic modulus of the struts (the solid material from which scaffolds are formed) and a constant related to pore geometry. Gorczyca et al. [6] proved that when scaffolds were in the swollen state, the pores filled with water, and that pore size contributed more to mechanical strength than did the effect of the crosslinking reaction. Davidenko et al. [12] detected a significant decrease in Young's modulus of collagen-based scaffolds (~ 65%) following 10 days of incubation in water. Xingang et al. [13] found that scaffolds based on hydrophilic materials such as collagen and chitosan exhibited significantly decreased mechanical strength than did scaffolds based on hydrophobic materials such poly(L-lactide-co-glycolide). A decrease in stiffness was observed following hydration by Varley et al. [10], probably caused by the weakening of hydrogen bonds within the molecular structure of the collagen, as illustrated by the Young's modulus values obtained (~ 5–10 kPa for the dry and ~ 0.5–1 kPa for the hydrated forms). Kane et al. [14] determined a compressive modulus of up to ~1 MPa following the hydroxyapatite reinforcement of collagen scaffolds which were prepared by means of compression moulding with paraffin microspheres employed as the porogen. Moreover, the compressive modulus was found to be at least one order of magnitude greater than for comparable freeze-dried scaffolds.

In comparison to dry scaffolds, a major decrease in stress and significantly extended stress–strain curve plateau zones were registered with respect to the hydrated samples [5, 16]. The swollen scaffolds exhibited reduced compressive strength while the ability to respond to compressive deformation increased, which led to significant differences in the stress–strain curves compared to those of the dry scaffolds. Jose et al. [16] studied the effect of material composition on the final properties of the

scaffold. They proved that varying the collagen concentration, while keeping all the other parameters constant, resulted in an increase in the amount of absorbed water in the scaffolds and, thereby, increased the hydrophilicity of poly (lactide-co-glycolide) scaffolds. Uni-axial tensile testing revealed a decrease in modulus with increasing collagen content. It is evident that the content of hydrophilic components in the composite is a further key factor influencing the final properties of scaffolds [12, 17-20]. The hydrated state much better approximates to the *in vivo* situation. However, the measurement of composite properties in this state, such as porosity and mechanical properties, is frequently neglected [19, 21-25] and often not determined at all [26].

The study described herein concerns follow-up research to a study previously published by Suchý et al. [27] which described the development of a composite material based on natural collagen, polylactide electrospun nano-fibres and natural calcium phosphate nano-particles, and compared the effect of different cross-linking conditions on the structural and mechanical properties in the dry state as well as the swelling ratio and mass loss of cross-linked scaffolds; the study also included an investigation of human mesenchymal stem cells adhesion and proliferation within the scaffolds. The aim of the present work, however, is to describe the study of the influence of eight differing scaffold material compositions, focusing on collagen content and their final properties such as internal structure, porosity and mechanical properties in both the dry and hydrated states. It was anticipated that the differences in physical properties following hydration would represent a significant limiting factor for the seeding, growth and differentiation of mesenchymal stem cells and the overall applicability of such hydrophilic materials.

2. Materials and methods

2.1. Materials

A collagen (type I, calf skin, VUP Medical, Czech Republic) solution (5 wt%) was prepared by means of the swelling of collagen in deionised water and homogenised by means of a disintegrator (10,000 rpm, 10 min).

Poly DL-lactide (PURASORB PDL05, Purac, NE) sub-micron fibre (diameter 275–300 nm, lower—upper quartile) mats were prepared by means of electrospinning from a 10 wt% chloroform solution (Nanospider NS LAB 500, Elmarco, Czech Republic). Prior to the preparation of the scaffolds, PDLLA fibres were homogenised using a disintegrator for 5 min at 14 000 rpm (DI 18, IKA) in distilled water, frozen at −15°C for 24 h and subsequently lyophilised at −105°C and at a pressure of approximately 1.3 Pa.

Bioapatite was obtained from chemically- and thermally-treated bovine bone inspired by Murugan et al [28]. The cortical bovine bone was sliced into pieces of the required size. Macroscopic soft tissue and marrow impurities were removed by means of heating with a 2% NaCl solution at 150°C and a pressure of 0.2 MPa in autoclave followed by degreasing in an acetone–ether mixture (ratio 3:2) for 24 h. The bone samples were then treated with 4% NaOH solution at 70 °C for 24 h. The product was washed with deionised water until a neutral reaction was obtained. The chemically-treated bone samples were calcined overnight at 600°C under atmospheric pressure and ambient humidity. The product was finally washed in deionised water and dried at 105°C to constant weight.

2.2. Scaffold preparation

Composite scaffolds based on a collagen matrix (COL), poly DL-lactide sub-micron fibres (PDLLA), bioapatite (bCaP) and sodium hyaluronate (HYA) powder (HySilk, Contipro, Czech Republic) were prepared in 8 material variations (Fig. 1) employing the following procedure: An aqueous collagen dispersion (up to 4 wt%) was prepared by means of the swelling of collagen in deionised water, homogenised using a disintegrator (10 000 rpm, 10 min) and left for 60 min at a temperature of 20°C.

Water, acting as the porogen, represented 90 wt.% of the scaffolds. Collagen dispersion was further modified by means of PDLLA fibres, bCaP particles and HA powder; final homogenisation was performed using a disintegrator (6 500 rpm, 10 min). The resulting dispersion was placed in separate cylindrical containers with an inner diameter of 10 mm, frozen at −70°C for 3 h and then lyophilised. The collagen part of the scaffolds was cross-linked by EDC/NHS (N-(3-dimethylamino propyl)-N'-ethylcarbodiimide hydrochloride / N-hydroxysuccinimide) at a weight ratio of 4:1 in ethanol solution (95 wt.%). EDC and NHS (Sigma Aldrich, Germany) were used as received. Following a reaction period of 24 h at 37°C, all the scaffolds were washed in 0.1 M Na_2HPO_4 (2 × 45 min), rinsed using deionised water (30 min), frozen at −30°C for 5 h and lyophilised.

2.3. Scaffold characterisation in the dry and hydrated states

The morphology of the scaffolds was investigated by means of micro-CT analysis in both the dry and hydrated states. Micro-CT scans were acquired using SkyScan 1272 (Bruker, Belgium). All the specimens were scanned in air in the dry state. The hydrated specimens were scanned (immersed in deionised water in closed plastic tubes) at time intervals of 4, 8, 24 and 48 hours following initial hydration. Prior to scanning in the hydrated state, the samples were X-ray contrasted using Lugol's solution (3.33 g/L iodine, 6.66 g/L potassium iodide). The samples were inserted into silicon tubes with an inner diameter of 6 mm, and 20 ml of Lugol's solution was applied using a linear pump in one direction (20 ml/hour) and repeated in the reverse direction after a 30-minute delay. Following contrasting, the samples were gently washed with deionised water and inserted into sample containers with deionised water. All the scans were conducted under the following scanning parameters: 4 um pixel size, source voltage 60 kV, source current 166 μA, 0.25 mm Al filter, frame averaging (2), 180° rotation. The scanning time was approximately 1 hour for each specimen. The flat-field correction was updated prior to each acquisition. Cross-section images were reconstructed from projection images taken with NRecon software (Bruker, Belgium) and using a modified Feldcamp algorithm with the adequate setting of the correction parameters (misalignment, ring artefact and

beam hardening) so as to reduce the effect of computed tomography artefacts. Visualisations were acquired by means of DataViewer (2D cross-section images) and CTVox (3D images; Bruker, Belgium). Scaffold structure analysis, including porosity analysis, was performed by means of CTAn (Bruker) in 3D using a sphere fitting algorithm following image binarisation. The VOI (volume of interest) subjected to analysis was set within the scaffold structure and was cylindrical in shape (5 mm in height and 5 mm in diameter) and excluded the superficial parts of the specimen which might have been altered as a consequence of the treatment of the specimen.

2.4. Mechanical behaviour in the dry and hydrated states

In order to describe the mechanical behaviour of the scaffolds in the dry and hydrated states, compression tests were performed by means of the adaptation of the ISO 13314 standard [29] which refers to the mechanical testing of porous and cellular metals. The mechanical properties of the scaffolds were measured on both dry samples and samples hydrated in α MEM medium (Life Technologies, USA) for 24 and 48 hours. Six cylindrical samples with a diameter of 6.2 mm and a length of 8.5 mm were tested in each group (i.e. a sample length to diameter ratio of approximately 1:4). Plateau stress, elastic gradient and energy absorption were determined using an MTS Mini Bionix 858.02 system (MTS, USA) equipped with 10 N and 100 N load cells. The measurements were carried out at a constant crosshead speed of 3.0 mm min^{-1} (deformation rate approx. 5 10^{-3} s^{-1}, i.e. in the range of 10^{-3} and 10^{-2} s^{-1}). The stress-strain curves obtained were used to determine the mechanical properties as follows: Plateau stress (σ_{pl}) was defined as the arithmetical mean of the stresses between 20% and 30% compressive strain. The elastic gradient ($E_{\sigma 20–\sigma 70}$) was calculated as the gradient of the elastic straight lines determined by elastic loading and unloading between stresses of 70% and 20% of the σ_{pl}. Energy absorption (W) was calculated as the area under the stress-strain curve up to 50% strain. Finally, energy absorption efficiency (We) was calculated as energy absorption divided by the product of the maximum compressive stress within the strain range and the magnitude of the strain range. Plateau stress and elastic gradient represent the closest concepts to that of yield stress and Young's

modulus respectively, which are employed for solid materials [30]. In order to simplify the comparison of our results and the results of other studies, we assumed that plateau stress represents compression strength and that elastic gradient represents the modulus of elasticity under compression [30-32].

2.5. Hydraulic permeability measurement

Permeability at different time points was measured for each type of scaffold (at least 6 specimens per group), applying a constant flow rate (*Q*) and acquiring a pressure drop throughout the thickness of the scaffold *(ΔP*). Cylindrical specimens with a diameter of 5.5 mm and a thickness of 5 mm were used for testing purposes. The experimental layout (adapted from a previous study [33], Supplement 1) consisted of: i) a perfusion chamber hosting a deformable silicone-made cartridge (Sylgard 184 Dow Corning Corporation) containing the scaffold and ensuring confined-flow perfusion; ii) a peristaltic pump (Ismatec IPC-N, Cole-Parmer GmbH) for ensuring fluid flow through the scaffold; and iii) an I/O acquisition system (NIDAQcard-6036E and LabViewTM, National Instruments) which was employed for the real-time monitoring and acquisition of pressure values. A Press-S-000 (PendoTECH, USA) pressure sensor provided inflow pressure values, while outflow pressure values were taken at atmospheric pressure in the adopted set-up (Supplement 1).

Permeability measurements were performed in a water bath at a constant temperature (37°C), and deionised water was used as the working fluid. Several flow rate values were applied, increasing *Q* in the range 100-1000 µl/min (in steps of 100 µl/min). The *ΔP* measurements were repeated three times. The *ΔP-Q* data was registered after 5 minutes of hydration, allowing the estimation of the permeability at the starting point (K_0) following 4 (K_4), 8 (K_8) and 24 hours (K_{24}) from the starting point. A constant flow rate of 100 µl/min was maintained across the scaffold between the two subsequent measurement sessions. Permeability [m^2], based on Darcy's Law, was calculated using the following equation: $K = \frac{\mu\, t}{\mathrm{A}\, m}$, where µ is the fluid viscosity, *t* is the mean scaffold thickness, A is the cross-sectional area and *m*

is the slope of the linear interpolation of the *ΔP-Q* data acquired at different *Q* values for each specimen.

2.6. Scaffold degradation

The *in vitro* degradation of the scaffolds was evaluated by means of the determination of mass loss and swelling ratio. The experiment aimed to simulate *in vitro* test conditions—the samples were immersed in a fully supplemented α MEM medium and incubated in conical flasks at 37°C and a 5% CO_2 atmosphere (DH CO_2 incubator, Thermo Scientific) for 24 and 48 hours and for 30 days. All the scaffolds were washed with deionised water, frozen at −30°C for 5 h and lyophilised. The extent of *in vitro* degradation was calculated according to the following equation: $D = \frac{W0-Wt}{W0}$, where *D* is the mass loss, W_o is the initial dried weight of the sample and W_t is the dried weight of the sample following degradation (*n = 3*). The swelling ratio (E_{sw}) was calculated using the following equation: $Esw = \frac{Wsw-W0}{W0}$, where *Wo* is the initial dried weight of the sample and W_{sw} is the weight of the swollen sample (*n = 3*). The weight of the swollen samples was measured following the removal of each sample from the medium and after a 1 min delay and the removal of any excessive medium surrounding the sample.

Collagenase degradation tests were performed according to [34]. Lyophilised scaffolds were immersed in 0.1 M Tris–HCl containing 50 mM$CaCl_2$ and incubated at 37°C for 0.5 h. Subsequently, 0.1 M Tris–HCl containing 50 units of collagenase from Clostridium histolyticum, Type I, (Sigma–Aldrich) was added to the solution and the scaffolds were immersed in the bath at 37°C for 1 h. The reaction was terminated by means of the addition of 0.25 M EDTA and cooling on ice. The samples were rinsed with deionised water three times and then immersed in ethanol for 3 h. They were then rinsed with deionised water, frozen at −30°C for 5 h and lyophilised. The mass loss was calculated from the dry weight prior to and following enzyme digestion (*n=3*).

The structure of the scaffolds (*n=4*) following collagenase degradation was evaluated by means of attenuated total reflection infrared spectrometry (FTIR) using a Protégé 460 E.S.P. infrared spectrometer (Thermo Nicolet Instruments, USA) equipped with an ATR device (GladiATR, PIKE Technologies, USA) with a diamond crystal. All the spectra were recorded in absorption mode at a resolution of 4 cm^{-1} and 128 scans in a spectral region of 4000 - 400 cm^{-1}. The areas of the bands (integral absorbencies) were determined using OMNIC 7 software.

2.7. Statistical analysis

The statistical analysis was performed using statistical software (STATGRAPHICS Centurion XV, StatPoint, USA). Normally distributed numerical data was expressed as the arithmetical mean, SD (standard deviation). The normality of the data was confirmed using the Shapiro-Wilk and Chi-Squared tests. Outliers were identified via the Grubbs and Dixon tests. Non-normally distributed numerical data was expressed as the median, IQR (interquartile range). For normally distributed data, statistically significant differences were checked by means of the parametric analysis of variance (F-test); Student-Newman-Keuls (SNK) and Fisher's least significant difference (LSD) post hoc tests were employed after confirming the following assumptions: i) the distribution derived from each of the samples was normal and ii) the variances of the population of the samples were equal to one another (assumption of homoscedasticity). Homoscedasticity was controlled for using the Levene, Bartlett and Cochran tests. Non-parametric analysis was conducted when either of the two above-mentioned assumptions were violated, followed by the performance of the Kruskal-Wallis test for multiple comparisons and the Mann-Whitney W test as a post hoc test. Statistical significance was accepted at $p \leq 0.05$.

3. Results

3.1. Scaffold characterisation

Micro-CT analysis in the dry state was performed for each type of scaffold (*n=8*) (Fig. 2). The analysis was performed in 3D using CTAn. The main structural parameters consisted of open porosity volume

(percent), closed porosity volume (percent) and pore size which was assessed in 3D based on the structure thickness distribution determined via the sphere-fitting algorithm.

The morphology parameters obtained by means of micro-CT analysis are presented in Fig. 3. Pore size in the dry state varied for each type of scaffold, with concern to which the respective types can be divided into 3 groups with similar values: low pore size (scaffolds 1, 2, 4 and 6), medium pore size (scaffolds 5, 7 and 8) and large pore size (scaffold 3). Open porosity values (OP = volume of the open pores / total VOI volume) ranged from 82.3% to 87.81%. Open pores were defined as spaces within the scaffold structure which displayed a connection with the space outside the object. All the scaffold types provided a high degree of open porosity. Closed porosity values (CP = volume of closed pores / scaffold volume + the volume of closed pores) ranged from 0.01% to 0.06%. Scaffold volume was taken to mean the volume of scaffold material without the pores. Closed pores were defined as spaces completely surrounded by the scaffold structure with no connection in 3D with the surface of the scaffold. All the specimens exhibited a very low degree of closed porosity, thus suggesting a high degree of interconnected pores.

3.2. Mechanical behaviour in the dry and hydrated states

The mechanical properties of the scaffolds in the dry and hydrated states obtained in the study are provided in Figs. 4 to 7. The mechanical properties of composite scaffolds were influenced by their composition, namely the weight or volume fraction of particular components. In our case, it appears that the collagen matrix played an essential role in terms of mechanical behaviour in both the dry and hydrated states. In the dry state, the low amount of collagen (10-20 wt%) reduced the degree of stiffness (represented by the elastic gradient) to approx. 2 - 7 MPa and compressive strength (represented by plateau stress) to approx. 0.1 – 0.3 MPa. 30 - 40 wt% of collagen appeared to represent a sufficient amount so as to provide for the appropriate bonding of all the components of the scaffolds. This was represented by the stable level of stiffness (15 MPa) and compressive strength (0.5 MPa) of

samples 3 – 8; the differing weight fractions of PDLLA and bCaP did not exert a statistically significant effect on the mechanical properties (Fig. 4 and Fig. 5).

The elastic modulus of all eight samples decreased immediately following hydration (Fig. 4). This statistically significant drop was represented by an up to 100 times lower degree of stiffness. A further 24 hours of hydration was found to exert no significant effect on stiffness. A similar trend was evinced by the compressive strength of all the samples following hydration (Fig. 5). The plateau stress of all the samples decreased up to 10 times following 24 hours and remained stable after a further 24 hours. In contrast to previous findings, energy absorption efficiency (Fig.6) decreased only up to 20% following hydration. This parameter represents the ability of the material to effectively absorb deformation energy. A comparison of energy absorption efficiency in the dry and hydrated states indicated relatively low changes in the inner structure of the scaffolds following hydration.

3.3. Hydraulic permeability measurement and porosity in the hydrated state

The permeability of seventy-one scaffolds was tested (from *n=6* to *n=11* specimens for each of the eight scaffold types) and three measurements were performed for each scaffold immediately following a hydration period of 5 min (K_0), and after 4 (K_4), 8 (K_8) and 24 (K_{24}) hours. The overall K_0 mean permeability was found to be in the range 2 x 10^{-13} (type 4) and 8.5 x 10^{-13} m^2 (types 1 and 7). Permeability measurements over time revealed the stable behaviour of the scaffolds irrespective of scaffold type with no significant differences. Notably, scaffold type 2 exhibited a pronounced increase in the permeability value after 4 hours (Fig. 7, left). The statistical comparison of the 8 types of scaffold revealed a number of significant differences (Fig. 7, right); importantly, scaffold type 1 exhibited very high permeability values (especially after 24 hours) which differed significantly from the other scaffold type values (Fig. 7 P1, right).

In order to provide for the illustration of the influence of hydration on the inner structure, the porosity of selected samples with different compositions (scaffolds 3, 6 and 8) was measured by means of micro-CT 3D analysis. Three types of scaffold were subjected to analysis during hydration in deionised water (see Fig. 8).

One specimen was chosen from each group of scaffolds (based on differing pore size as mentioned above in 3.1) (Fig. 9). Analysis was performed in the same way as in the dry state. The time intervals were 0 (dry state), 4, 8 and 24 hours following initial hydration. An initial reduction in open porosity (4 hours) to below the dry state value was followed by a slight increase in this parameter with respect to all the specimens. Closed porosity initially slightly increased (4 hours) with concern to all the specimens, following which a reduction was observed concerning specimens 3 and 8. Specimen 6 maintained the increased level of closed porosity.

3.4. Scaffold degradation

The *in vitro* degradation rates of 8 scaffold material compositions in α MEM medium expressed as mass loss and swelling ratios are summarised in Figs. 10 and 11. Negative values of degradation (Fig. 10) indicate a weight increase. As can be seen from Fig. 10, the increment size increased over time. The swelling ratio of scaffolds 1 and 6 remained almost unchanged over the 24-day incubation period. All the other scaffolds exhibited an increment in the swelling ratio, which increased according to the period of incubation. This phenomenon was most apparent with respect to scaffolds 7 and 8.

The mass loss of individual material compositions after 1 hour of collagenase treatment and their comparison with non-crosslinked collagen (NC) is summarised in Fig. 12. Degradation was expressed as wt% loss of the composite and this was recalculated to wt% loss of collagen in the scaffold. Statistically significant differences are evident with respect to scaffolds 1, 2 and the sample NC.

Scaffolds 3-8 exhibited a composite loss of up to 1.5 wt% and a collagen loss of ~ 4 wt%. Scaffold 1 achieved an almost 8 wt% composite loss and a significant 78 wt% collagen loss.

FTIR spectroscopy was employed in order to clarify these somewhat anomalous results. Changes in the integral absorbances of individual scaffold components (PDLLA, COL and bCaP) were determined before and after 1 hour of collagenase treatment (Fig. 12). It was anticipated that these ratios would explain the changes in the composition of the composite following degradation. The strong band ~1750 cm^{-1} belonging to PDLLA, the amide I band (~1650 cm^{-1}) typical for collagen and the ν_4 PO_4 domain (510-660 cm^{-1}) related to apatites were used for the calculation of the ratios of the integral absorbances of individual scaffold components (PDLLA/COL and bCaP/COL). The strongest band ~1030 cm^{-1} belonging to the apatites was not used for calculation purposes due to a partial overlap with the shoulder of the PDLLA band. The medians of the integral absorbance of PDLLA and bCaP (Fig. 12) related to COL remained the same or decreased following degradation. Statistically significant differences were most apparent with respect to scaffolds 1 and 7 in the case of the bCaP/COL ratio and scaffold 8 in the case of the PDLLA/COL ratio.

4. Discussion

Eight scaffolds of different composition were prepared and their properties in both the dry and wet forms were evaluated. It was supposed that each composition would exert a different effect on the properties of the scaffolds according to the collagen, calcium phosphate and polylactide acid fibre ratio. In spite of a few differences in some of the results obtained from the application of various methods, the overall structure and mechanical stability were found to be similar.

Scaffold permeability, combining the topological properties of the 3D structure (such as scaffold porosity, pore size, interconnectivity and tortuosity), plays an important role in determining overall scaffold performance in terms of fluid mass transport (i.e. nutrients and oxygen), waste removal and

cell penetration to the core of the scaffold [35]. Hence, defining the optimal scaffold permeability range provides a challenge in terms of the potential use of such scaffolds in tissue engineering applications. The permeability of the 8 types of scaffold presented in this study (order of magnitude of 10^{-13} m^2) is comparable to that reported in literature for collagen-based scaffolds [10, 36-38] and falls between the permeability values obtained for trabecular (range from 10^{-10} to 10^{-9} m^2 [39]) and cortical bone (10^{-17} m^2 [40]). The scaffold composition and permeability data indicated that both collagen and apatite content contributed slightly towards determining scaffold permeability at time 0. Briefly, i.e. during the time that the collagen content inversely affected scaffold permeability, apatite content directly influenced the hydraulic behaviour of the scaffolds (Fig. 1 and Fig. 8, right panel). The temporal evolution of scaffold permeability was also investigated up to 24 hours, the results revealing the stable behaviour of all 8 scaffold types. These results are in agreement with the morphological measurement results (pore size, open porosity and closed porosity) obtained via micro-CT (Fig. 3 and Fig. 10). Importantly, this morphological data revealed that scaffold hydration does not affect open porosity, thus guaranteeing stable permeability behaviour over time.

With respect to the swelling and permeability data at 24 hours, an opposite relationship between the swelling ratio (Fig. 12, right panel) and the permeability measurement results (Fig. 8, right panel) was observed. High swelling ratio values corresponded to lower permeability values (i.e. types 2, 4 and 6) and *vice versa* (i.e. types 3, 5, 7 and 8). In addition, type 1 exhibited higher swelling ratio values and high permeability; however, these values were not statistically significant.

The weight increase observed during degradation in α MEM (Fig. 11) can be explained by means of the adsorption of various components (proteins, saccharides, vitamins and salts) contained in the α MEM medium. The weight increments increased with incubation time, which was also observed with concern to swelling (Fig. 12); however, after 576 hours the composites differed from each other less than they did after just 24 and 48 hours of incubation. The smallest swelling values were exhibited by

samples 7 and 8, which contained over 50 wt.% of bCaP. Degradation occurred (albeit not particularly apparent) simultaneously to adsorption. The mass loss values of all the scaffolds varied only in terms of units of % and, therefore, it is not possible to state explicit conclusions in this respect.

Conversely, collagenase degradation exhibited the highest rate of collagen degradation with respect to scaffold 1. Scaffolds 3-8 exhibited a difference between the degradation of the composite and that of the collagen of up to 4%, while for scaffold 2 this difference was 7% and for scaffold 1 as much as 70%. These discrepancies can be explained by the low content of collagen acting as a binder holding the scaffolds together. The integral absorbance of PDLLA and bCaP (Fig. 13) related to COL remained the same or decreased following degradation, although these components were not attacked by collagenase. It follows that these components are released from the scaffold. The lower degree of scaffold consistency allows for the enhanced accessibility of collagenase to the collagen and hence the easier degradation thereof. These changes were most evident with respect to scaffolds 1 and 2 which had the lowest collagen content.

Collagen-like peptides tend to adopt the polyproline II helix and have *trans* isomers of their peptide bonds with dihedral angles ($\psi \approx 150^\circ$, $\phi \approx -75^\circ$). *Trans* configuration for the peptide bond is favoured over the *cis* form by 1.3 kcal/mol. The potential energy of the system is a function of the dihedral angle. Gautieri et al. [41] performed the Ramachandran analysis of a fully equilibrated full-atomistic collagen microfibril system in both hydrated (wet) and dehydrated (dry) conditions. They proved that hydrated collagen microfibril lies within a region of the diagram ($\psi \approx 150^\circ$, $\phi \approx -75^\circ$) characteristic of the polyproline II chain and thus of collagen-like peptides. However, an analysis of the dehydrated collagen microfibril system revealed a broader range of dihedral angles indicating a certain level of molecular unfolding. Dehydrated microfibrils exhibit higher dihedral energy than they do in the hydrated state. This suggests that in the dehydrated microfibril the deformation mechanism initially involves primarily the straightening of the collagen molecules and not the stretching of the molecules. Conversely, the

hydrated state allows collagen molecules to adopt conformations with maximal entropy, and the system exhibits a low level of dihedral (potential) energy. However, the mechanical properties are highly scale dependent. A direct numerical comparison suggests differences in Young's modulus of from several GPa for a single molecule to a few hundred MPa for collagen microfibrils, representing a striking change in the mechanical properties at different hierarchical levels [41]. The system studied herein was much more complicated since the collagen was chemically cross-linked. The presence of covalent inter-molecular cross-links increased adhesion at the ends of each molecule [42]. In addition, the system had a high porosity level and elastic deformation occurred primarily via the bending of slender structural elements, such as the cell walls. This allowed for significant deflections under low applied loads – i.e. the generation of low levels of stiffness – and this makes up the basis of many types of (highly compliant) fibre network materials [10].

Due to the possible future application of scaffolds, it is suggested that the results also be considered with respect to the cell perspective. The results indicate that the combination of materials, the ratio of material components, fibre organisation into higher structural units and specific environmental conditions determine the surface area, porosity, swelling and degradation of the composite. All of them are capable of fundamentally determining cell adhesion as well as overall function [43, 44]. The results revealed that bCaP had no significant effect on the mechanical properties of the scaffolds tested. Thus, from the cell perspective, scaffolds with a higher bCaP content may be more preferable. However, the results also showed that the mechanical properties of the scaffolds were directly influenced by the presence of collagen. The results confirmed the previously observed dependency between collagen and the mechanical properties of the scaffolds and revealed the opposite proportionality between collagen content and the stiffness of the material. Therefore, scaffolds with a collagen content in the scaffold of around 30-40% would appear to be more appropriate in terms of predicted cell adhesion. If we take this result together with the afore-mentioned potential biological benefits of bCaP, it can be assumed that the optimum mechanical properties in terms of cell application

will be provided by scaffolds with a higher bCaP content and a collagen content of around 30-40%. That said, a more specific determination of the best ratios of both components in the scaffold can be provided only by means of a biological evaluation. The results revealed the elastic deformation of the tested scaffolds, which indicated a low degree of stiffness. In general, material stiffness determines the generation of cell traction forces and, subsequently, affects changes in cell morphology and movement and cell differentiation [45-47]. With respect to bone tissue engineering, scaffolds with the highest levels of rigidity (lowest elasticity) are recommended with concern to cell osteo-differentiation.

The results also revealed variability with respect to other factors which may crucially impact cell behaviour - swelling, porosity and pore-size [48]. The observed general elevation of the swelling rate following hydration may be significantly affected by the scaffold environment, thus by the presence of a cultivation medium (specifically αMEM supplemented with foetal bovine serum (FBS)). Moreover, water binding by medium proteins (originating in FBS), in connection with other scaffold components (which differed with respect to all the scaffolds tested), may have resulted in differences in the swelling rate of the tested scaffolds [49, 50]. Therefore, the optimal scaffolds for cell application would appear to be those that change only slightly during the first 24h of incubation (scaffolds 1 and 6) or those scaffolds with the lowest swelling ratio (scaffolds 7 and 8). From the viewpoint of permeability, which is directly related to swelling (as the results indicate) and which is important with respect to cell nourishment and penetration, those scaffolds displaying higher permeability would appear to be more suitable (i.e. scaffolds 3, 5, 7 and 8).

Swelling is also closely related to pore size and porosity. From the perspective of biomaterial engineering and the development of artificial extracellular matrices, we determined no clear results concerning the ideal pore size and porosity of cells [51, 52]. The variable results suggest, therefore, the importance of the context of the entire scaffold. The scaffold porosity results predicted a degree of porosity of 85% and a high degree of interconnected pores, both of which are important factors in

terms of cell nutrition and cell migration. When compared to native bone, the scaffolds are close to cortical bone with respect to pore size (porosity 3–12%, pore-size 100–200 µm); however, the degree of porosity indicates a closer approximation to trabecular bone (a high porosity of around 50–90%, pore size diameters of up to 1 mm) [53, 54]. Thus, from the perspective of the native state of bone, the scaffolds have the potential to provide an artificial bone matrix. In addition, the aim of the scaffold is to allow cells to adhere within the structure of the scaffold and to remain in this position for subsequent proliferation and differentiation.

Taken together, therefore, the results acquired are important in terms of the typing of the most appropriate scaffolds for biological *in vitro* and *in vivo* evaluation. The results must be considered with respect to future medical application, the type of cells used, cell requirements and the cell application method [48]. Further, the results demonstrate the importance of detailed mechanical testing under conditions which best approximate to bio-application *in vitro* or *in vivo* conditions, which may assist in the typing of biomaterial for advanced biological analysis purposes.

5. Conclusions

The pore size, permeability and mechanical properties of tissue engineering scaffolds influence migration and cell growth in the context of cell seeding and further cultivation. Permeability connects the structural properties of the 3D structure and affects the hydration of the scaffold. Moreover, depending on the composition of the material, the hydration of such highly-porous structures may further influence mechanical behaviour and porosity due to swelling. This mechanism is particularly obvious in the case of scaffolds prepared based on the use of hydrophilic materials such as collagen, gelatine and chitosan as natural polymers. This study evaluated both the mechanical and structural properties of scaffolds based on collagen, poly(DL-lactide) and calcium phosphate particles with 8 different material compositions in the dry and hydrated states. Hydration, simulating the conditions of cell seeding and cultivation up to 48 hours and 576 hours, was found to exert a minor effect on the

morphological parameters such as pore size, open porosity, and on the permeability. The mass loss of individual scaffolds was detected only following the application of targeted enzymatic treatment by means of collagenase, with no indication of degradation in the cultivation media. Conversely, hydration had a major statistically significant effect on the mechanical behaviour of all the tested scaffolds with no effect according to the amount of collagen. The elastic modulus and compressive strength of all the scaffolds with 10-40 %wt of collagen decreased by ~95%. Despite a small change in the structural properties, this decrease confirms the importance of analysing scaffolds in the hydrated rather than the dry state since the former more precisely simulates the real environment for which such materials are designed. The measurement of scaffolds in the dry state is, however, useful with respect to the basic characterisation of the selection of preparation methods and chemical treatment; however, it is important that real conditions not be neglected, especially with concern to hydrophilic polymers.

Acknowledgements

This study was supported by a grant project awarded by the Ministry of Health of the Czech Republic (15-25813A). This publication is the result of the implementation of the "Technological development of post-doc programmes" project, registration number CZ.1.05/41.00/16.0346, supported by the Research and Development for Innovations Operational Programme (RDIOP), co-financed by European regional development funds and the state budget of the Czech Republic. The project was also supported by "Progres Q29/1LF, Ministry of Education, Youth and Sports of the Czech Republic" and GAUK no. 400215. We gratefully acknowledge the financial support provided for our work by the long-term conceptual development research organisation under project no. RVO: 67985891. Special thanks go to Darren Ireland for the language revision of the English manuscript.

References

[1] C. Jungreuthmayer, M.J. Jaasma, A.A. Al-Munajjed, J. Zanghellini, D.J. Kelly, F.J. O'Brien, Deformation simulation of cells seeded on a collagen-GAG scaffold in a flow perfusion bioreactor using a sequential 3D CFD-elastostatics model, Med. Eng. Phys. 31 (2009) 420–427.

[2] Doillon C.J., Whyne C.F., Brandwein S., Silver F.H., Collagen-based wound dressings: Control of the pore structure and morphology, J. Biomed. Mater. Res. 20 (1986) 1219–1228.

[3] F.J. O'Brien, B.A. Harley, I.V. Yannas, L. Gibson, Influence of freezing rate on pore structure in freeze-dried collagen-GAG scaffolds, Biomaterials 25 (2004) 1077–1086.

[4] Y. Zhu, H. Wu, S. Sun, T. Zhou, J. Wu, Y. Wan, Designed composites for mimicking compressive mechanical properties of articular cartilage matrix, J. Mech. Behav. Biomed. Mater., 36 (2014) 32 – 46.

[5] Y. Zhu, Y. Wan, J. Zhang, D. Yin, W. Cheng, Manufacture of layered collagen/chitosan-polycaprolactone scaffolds with biomimetic microarchitecture, Colloid. Surface. B, 113 (2014) 352–360.

[6] G. Gorczyca, R. Tylingo, P. Szweda, E. Augustin, M. Sadowska, S. Milewski, Preparation and characterization of genipin cross-linked porous chitosan–collagen–gelatin scaffolds using chitosan–CO_2 solution, Carbohyd. Polym. 102 (2014) 901– 911.

[7] Y. Elsayed, C. Lekakou, F. Labeed, P. Tomlins, Fabrication and characterisation of biomimetic, electrospun gelatin fibre scaffolds for tunica media-equivalent, tissue engineered vascular grafts, Mat. Sci. Eng. C 61 (2016) 473–483.

[8] N. Davidenko, J.J. Campbell, E.S. Thian, C.J. Watson, R.E. Cameron, Collagen–hyaluronic acid scaffolds for adipose tissue engineering, Acta Biomater. 6 (2010) 3957–3968.

[9] G. S. Offeddu, J. C. Ashworth, R. E. Cameron, M. L. Oyen, Structural determinants of hydration, mechanics and fluid flow in freeze-dried collagen scaffolds, Acta Biomater. 41 (2016) 193–203.

[10] M.C. Varley, S. Neelakantan, T.W. Clyne, J. Dean, R.A. Brooks, A.E. Markaki, Cell structure, stiffness and permeability of freeze-dried collagen scaffolds in dry and hydrated states, Acta Biomater. 33 (2016) 166–175.

[11] V. Beachley, X. Wen, Fabrication of nanofiber reinforced protein structures for tissue engineering, Mat. Sci. Eng. C 29 (2009) 2448–2453.

[12] N. Davidenko, C. F. Schuster, D. V. Bax, N. Raynal, R. W. Farndale, S. M. Best, R. E. Cameron, Control of crosslinking for tailoring collagen-based scaffolds stability and mechanics, Acta Biomater. 25 (2015) 131–142.

[13] W. Xingang, L. Qiyin, H. Xinlei, M. Lie, Y. Chuangang, Z. Yurong, S. Huafeng, H. Chunmao, G. Changyou, Fabrication and characterization of poly(L-lactide-co-glycolide)knitted mesh-reinforced collagen–chitosan hybrid scaffolds for dermal tissue engineering, J. Mech. Behav. Biomed. Mater., 8 (2012) 204 – 215.

[14] R.J. Kane, H.E. Weiss-Bilka, M.J. Meagher, Y. Liu, J.A. Gargac, G.L. Niebur, D.R. Wagner, R.K. Roeder, Hydroxyapatite reinforced collagen scaffolds with improved architecture and mechanical properties, Acta Biomater. 17 (2015) 16–25.

[15] D. Yin, H. Wu, C. Liu, J. Zhang, T. Zhou, J. Wu, Y. Wan, Fabrication of composition-graded collagen/chitosan–polylactide scaffolds with gradient architecture and properties, React. Funct. Polym. 83 (2014) 98–106.

[16] M.V. Jose, V. Thomas, D.R. Dean, E. Nyairo, Fabrication and characterization of aligned nanofibrous PLGA/Collagen blends as bone tissue scaffolds, Polymer 50 (2009) 3778–3785.

[17] T. Arahira, M. Todo, Variation of mechanical behaviour of β-TCP/collagen two phase composite scaffold with mesenchymal stem cell in vitro, J. Mech. Behav. Biomed. Mater. 61 (2016) 464 – 474.

[18] J. Elango, J. Zhang, B. Bao, K. Palaniyandi, S. Wang, W. Wu, J. S. Robinson, Rheological, biocompatibility and osteogenesis assessment of fish collagen scaffold for bone tissue engineering, Int. J. Biol. Macromol. 91 (2016) 51–59.

[19] R. Tylingo, G. Gorczyca, S. Mania, P. Szweda, S. Milewski, Preparation and characterization of porous scaffolds from chitosan-collagen-gelatin composite, React. Funct. Polym. 103 (2016) 131–140.

[20] R. Parenteau-Bareil, R. Gauvin, S. Cliche, C. Gariépy, L. Germain, F. Berthod, Comparative study of bovine, porcine and avian collagens for the production of a tissue engineered dermis, Acta Biomater. 7 (2011) 3757–3765.

[21] A. Arora, A. Kothari, D. S. Katti, Pore orientation mediated control of mechanical behavior of scaffolds and its application in cartilage-mimetic scaffold design, J. Mech. Behav. Biomed. Mater. 51 (2015) 169 – 183.

[22] F. Ghorbani, H. Nojehdehian, A. Zamanian, Physicochemical and mechanical properties of freeze cast hydroxyapatite-gelatin scaffolds with dexamethasone loaded PLGA microspheres for hard tissue engineering applications, Mater. Sci. Eng. C 69 (2016) 208–220.

[23] E. Jeevithan, R. Jeya Shakila, A. Varatharajakumar, G. Jeyasekaran, D. Sukumar, Physico-functional and mechanical properties of chitosan and calcium salts incorporated fish gelatin scaffolds, Int. J. Biol. Macromol. 60 (2013) 262– 267.

[24] M.S. Kim, G.H. Kim, Electrohydrodynamic direct printing of PCL/collagen fibrous scaffolds with a core/shell structure for tissue engineering applications, Chem. Eng. J. 279 (2015) 317–326.

[25] T. Muthukumar, A. Aravinthan, J. Sharmila, N. S. Kim, J.-H. Kim, Collagen/chitosan porous bone tissue engineering composite scaffold incorporated with Ginseng compound K, Carbohyd. Polym. 152 (2016) 566–574.

[26] H. Cao, M.-M. Chen, Y. Liu, Y.-Y. Liu, Y.-Q. Huang, J.-H. Wang, J.-D. Chen, Q.-Q. Zhang, Fish collagen-based scaffold containing PLGA microspheres forcontrolled growth factor delivery in skin tissue engineering, Colloid. Surface. B 136 (2015) 1098–1106.

[27] T. Suchý, M. Šupová, P. Sauerová, M. Verdánová, Z. Sucharda, Š. Rýglová, M. Žaloudková, R. Sedláček, M. Hubálek Kalbáčová, The effects of different cross-linking conditions on collagen-based nanocomposite scaffolds—an in vitro evaluation using mesenchymal stem cells, Biomed. Mater. 10 (2015) 065008.

[28] Murugan R, Ramakrishna S, Panduranga Rao K, Nanoporous hydroxy-carbonate apatite scaffold made of natural bone, Mater. Lett. 60 (2006) 2844–2847.

[29] ISO, ISO13314: 2011 Mechanical testing of metals—ductility testing—compression test for porous and cellular metals, 2011.

[30] S.A. Yavari, R. Wauthle, J. van der Stok, A.C. Riemslag, M. Janssen, M. Mulier, J.P. Kruth, J. Schrooten, H. Weinans, A.A. Zadpoor, Fatigue behaviour of porous biomaterials manufactured using selective laser melting, Mater. Sci. Eng. C 33 (2013) 4849–4858.

[31] S.M. Ahmadi, G. Campoli, S.A. Yavari, B. Sajadi, R. Wauthlé, J. Schrooten, H. Weinans, A. Zadpoor, Mechanical behavior of regular open-cell porous biomaterials made of diamond lattice unit cells, J. Mech. Behav. Biomed. 34 (2014) 106–115.

[32] K. Bobe, E. Willbold, I. Morgenthal, O. Andersen, T. Studnitzky, J. Nellesen, W. Tillmann, C. Vogt, K. Vano, F. Witte, In vitro and in vivo evaluation of biodegradable, open-porous scaffolds made of sintered magnesium W4 short fibres, Acta Biomater. 9 (2013) 8611–23.

[33] M. Piola, M. Soncini, M. Cantini, N. Sadr, G. Ferrario, G.B. Fiore, Design and functional testing of a multichamber perfusion platform for three-dimensional scaffolds, Sci. World. J. 2013 (2013) 123974.

[34] J. Kozłowska, A. Sionkowska, Effects of different crosslinking methods on the properties of collagen–calcium phosphate composite materials, Int. J. Biol. Macromol. 74 (2015) 397–403.

[35] J.M. Kemppainen, S.J. Hollister, Differential effects of designed scaffold permeability on chondrogenesis by chondrocytes and bone marrow stromal cells, Biomaterials 31 (2010) 279-287.

[36] F.J. O'Brien, B.A. Harley, M.A. Waller, I.V. Yannas, L.J. Gibson, The effect of pore size on permeability and cell attachment in collagen scaffolds for tissue engineering, Technol. Health Care 15 (2007) 3-17.

[37] Y. Wang, P.E. Tomlins, A.G. Coombes, M. Rides, On the determination of Darcy permeability coefficients for a microporous tissue scaffold, Tissue Eng. C 16 (2010) 281-289.

[38] M.M. Villa, L. Wang, J. Huang, D.W. Rowe, M. Wei, Bone tissue engineering with a collagen-hydroxyapatite scaffold and culture expanded bone marrow stromal cells, J. Biomed. Mater. Res. B 103 (2015) 243-253.

[39] W.J. Grimm, M.J. Williams, Measurements of permeability in human calcaneal trabecular bone, J. Biomech. 30 (1997) 743-745.

[40] D. Wen, C. Androjna, A. Vasanji, J. Belovich, R.J. Midura, Lipids and collagen matrix restrict the hydraulic permeability within the porous compartment of adult cortical bone, Ann. Biomed. Eng. 38 (2010) 558-569.

[41] A. Gautieri, S. Vesentini, A. Redaelli, M. J. Buehler, Hierarchical Structure and Nanomechanics of Collagen Microfibrils from the Atomistic Scale Up, Nano Lett. 11 (2011) 757–766.

[42] P. Fratzl, Collagen: Structure and Mechanics. Springer: New York, 2008.

[43] J. Venugopal, S. Ramakrishna, Applications of Polymer Nanofibers in Biomedicine and Biotechnology, Appl. Biochem. Biotechnol. 125 (2005) 147–158.

[44] M. Rampichová, J. Chvojka, M. Buzgo, E. Prosecká, P. Mikeš, L. Vysloužilová, D. Tvrdík, P. Kochová, T. Gregor, D. Lukáš, E. Amler, Elastic three-dimensional poly (ε-caprolactone) nanofibre scaffold enhances migration, proliferation and osteogenic differentiation of mesenchymal stem cells, Cell Prolif. 46 (2013) 23–37.

[45] A.J. Engler, S. Sen, H.L. Sweeney, D.E. Discher, Matrix Elasticity Directs Stem Cell Lineage Specification, Cell 126 (2006) 677–689.

[46] P. Kasten, I. Beyen, P. Niemeyer, R. Luginbühl, M. Bohner, W. Richter, Porosity and pore size of β-tricalcium phosphate scaffold can influence protein production and osteogenic differentiation of human mesenchymal stem cells: An in vitro and in vivo study, Acta Biomater. 4 (2008) 1904–1915.

[47] N.J. Walters, E. Gentleman, Evolving insights in cell–matrix interactions: Elucidating how non-soluble properties of the extracellular niche direct stem cell fate. Acta Biomater. 11 (2015) 3–16.

[48] K. Anselme, L. Ploux, A. Ponche, Cell/Material Interfaces: Influence of Surface Chemistry and Surface Topography on Cell Adhesion, J. Adhes. Sci. Technol. 24 (2012) 831-852.

[49] P. Dutta, S. Hajra, D.K. Chattoraj, Binding of water and solute to protein-mixture and protein-coated alumina, Indian J. Biochem. Biophys. 34 (1997) 449–460.

[50] B. Feng, J. Chen, X. Zhang, Interaction of calcium and phosphate in apatite coating on titanium with serum albumin, Biomaterials 23 (2002) 2499–2507.

[51] F.A. Akin, H. Zreiqat, S. Jordan, M.B.J. Wijesundara, L. Hanley, Preparation and analysis of macroporous TiO2 films on Ti surfaces for bone–tissue implants, J. Biomed. Mater. Res. 57 (2001) 588–596.

[52] T. Mygind, M. Stiehler, A. Baatrup, H. Li, X. Zou, A. Flyvbjerg, M. Kassem, C. Bünger, Mesenchymal stem cell ingrowth and differentiation on coralline hydroxyapatite scaffolds, Biomaterials 28 (2007) 1036–1047.

[53] D.M.L. Cooper, J.R. Matyas, M.A. Katzenberg, B. Hallgrimsson, Comparison of Microcomputed Tomographic and Microradiographic Measurements of Cortical Bone Porosity, Calcif. Tissue Int. 74 (2004) 437–447.

[54] T.M. Keaveny, E.F. Morgan, G.L. Niebur, O.C. Yeh, Biomechanics of Trabecular Bone, Annu. Rev. Biomed. Eng. 3 (2001) 307–333.

Captions

Fig. 1. Composition of the scaffolds in relation to the dry basis.

Fig. 2. Micro-CT visualisation of the 8 types of scaffolds in the dry state. Scale bar 1 mm.

Fig. 3. Pore size, closed porosity (CP) and open porosity (OP) [%] of the composite scaffolds in the dry state measured employing micro-CT 3D analysis. All the values exhibited statistically significant differences except those values designated by the symbol “o” (Mann-Whitney, 0.05).

Fig. 4. Elastic gradient (elastic modulus) of the scaffolds in the dry and hydrated (24 and 48 hours) states (median, IQR). Note that opposite axes have different scales. * denotes statistically significant differences (Mann-Whitney, 0.05) between different states (left) and different samples (right).

Fig. 5. Plateau stress (compressive strength) of the scaffolds in the dry and hydrated (24 and 48 hours) states (median, IQR). Note that opposite axes have different scales. * denotes statistically significant differences (Mann-Whitney, 0.05) between different states (left) and different samples (right).

Fig. 6. Energy absorption efficiency of the scaffolds in the dry and hydrated (24 and 48 hours) states (median, IQR). * denotes statistically significant differences (Mann-Whitney, 0.05) between different states (left) and different samples (right).

Fig. 7. Permeability after 5 min hydration (0 hours) and after 4, 8 and 24 hours (arithmetical mean, standard deviation). * denotes statistically significant differences (Mann-Whitney, 0.05) between different periods (left) and different samples (right).

Fig. 8. 3D visualisations of sections of scaffold specimen in the same position (type 3) in the dry state and at different time intervals following initial hydration. The inner structures of the scaffolds are visible including the pore walls, pore spaces and bCaP particles (higher X-ray density). Increased scaffold structure thickness can be observed as a result of hydration with an X-ray contrast agent, probably due to collagen swelling. Scale bar 500 μm.

Fig. 9. The pore size, closed porosity (CP) and open porosity (OP) [%] of the composite scaffolds in the dry state and hydrated for 4, 8 and 24 hours measured by means of micro-CT 3D analysis. All the values exhibit statistically significant differences except those values designated by the symbol “o” (Mann-Whitney, 0.05).

Fig. 10. The mass loss of the scaffolds following 24, 48 and 576 (24 days) hours of immersion in α MEM. * denotes statistically significant differences (Mann-Whitney, 0.05) between different states (left) and different samples (right).

Fig. 11. The swelling ratios of the scaffolds following 24, 48 and 576 (24 days) hours of immersion in α MEM. * denotes statistically significant differences (Mann-Whitney, 0.05) between different states (left) and different samples (right).

Fig. 12. Left: The mass loss of the scaffolds after 1 hour of collagenase treatment and their comparison with non-crosslinked collagen (NC). * denotes statistically significant differences (Mann-Whitney, 0.05) between the %wt. collagen medians. Right: Comparison of the ratio of integral absorbances PDLLA/COL and bCaP/COL of the original scaffolds and then following 1 hour of collagenase treatment. * denotes statistically significant differences (Mann-Whitney, 0.05) between the medians prior to and following collagenase degradation.

Figure 1

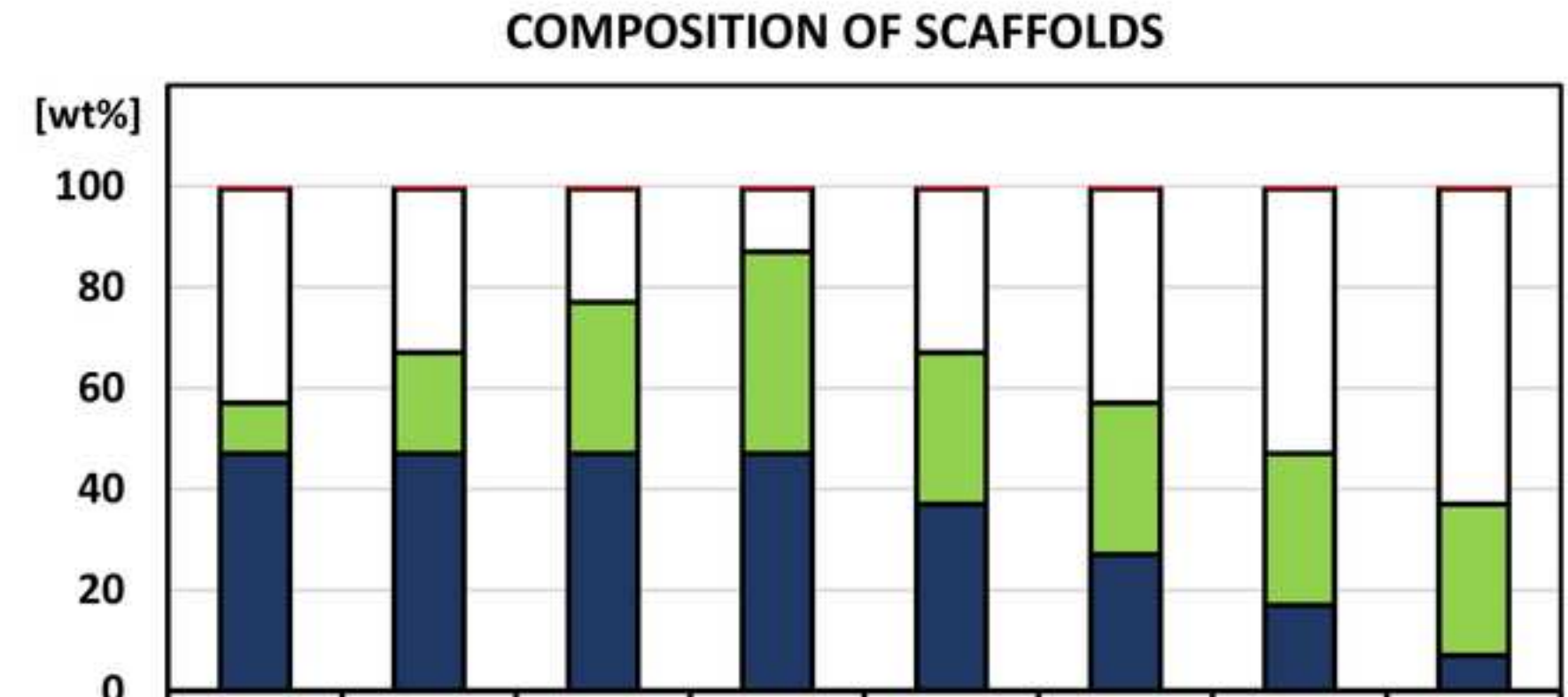

	1	2	3	4	5	6	7	8
HYA	0.5	0.5	0.5	0.5	0.5	0.5	0.5	0.5
bCaP	42.5	32.5	22.5	12.5	32.5	42.5	52.5	62.5
COL	10.0	20.0	30.0	40.0	30.0	30.0	30.0	30.0
PDLLA	47.0	47.0	47.0	47.0	37.0	27.0	17.0	7.0

Figure 2

Click here to download Figure FIGURE_2.tif

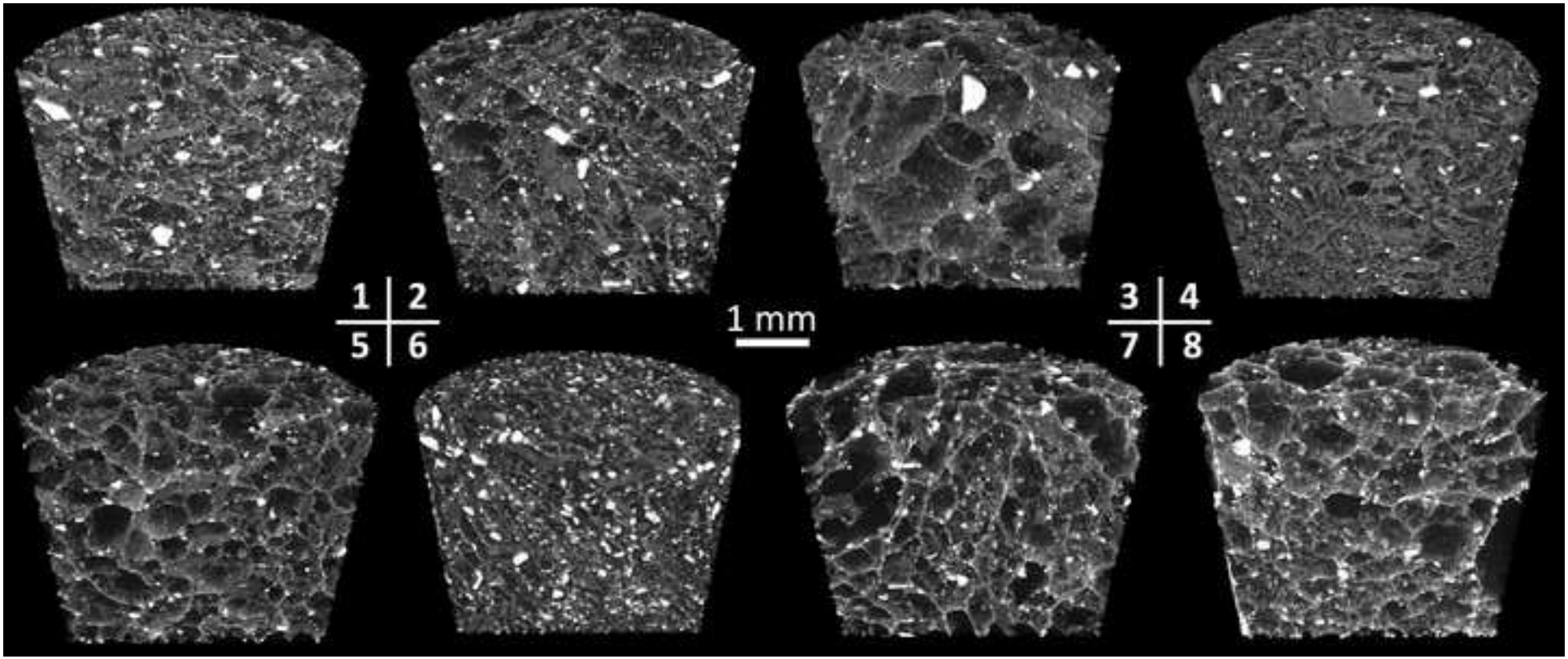

Figure 3

Click here to download Figure FIGURE_3.tif

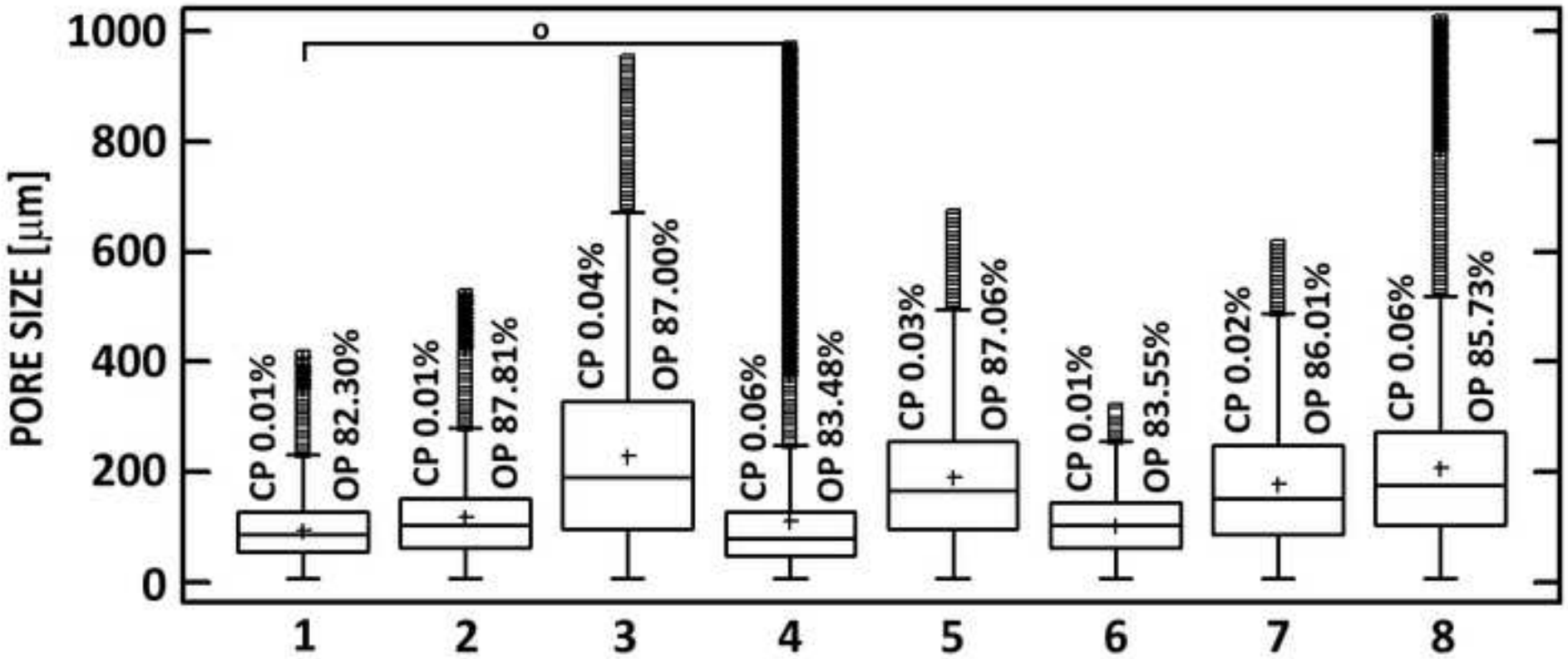

Figure 4

Click here to download Figure FIGURE_4.tif

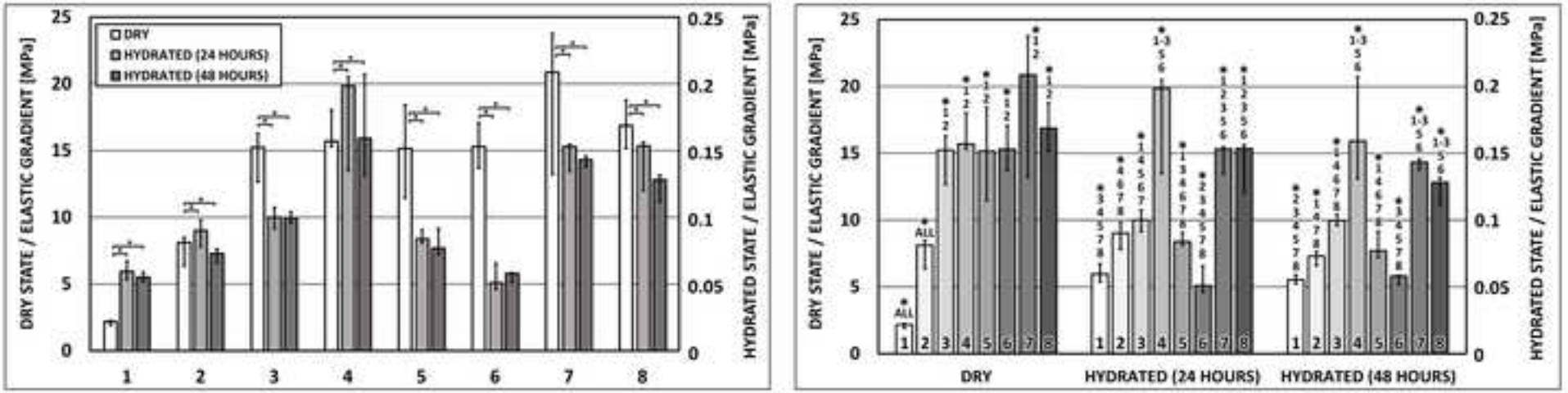

Figure 5

Click here to download Figure FIGURE_5.tif

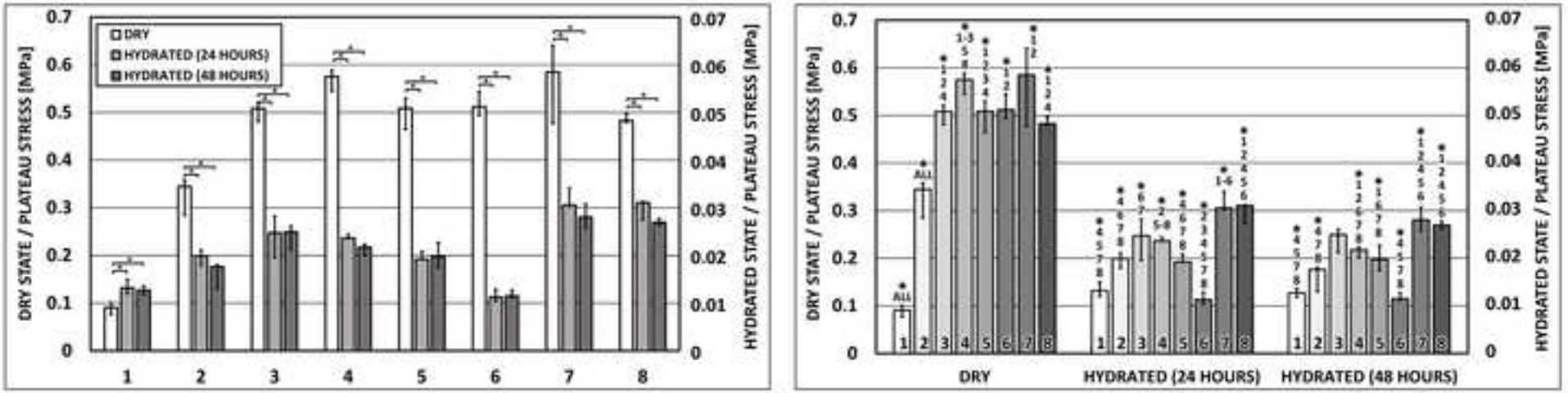

Figure 6

Click here to download Figure FIGURE_6.tif

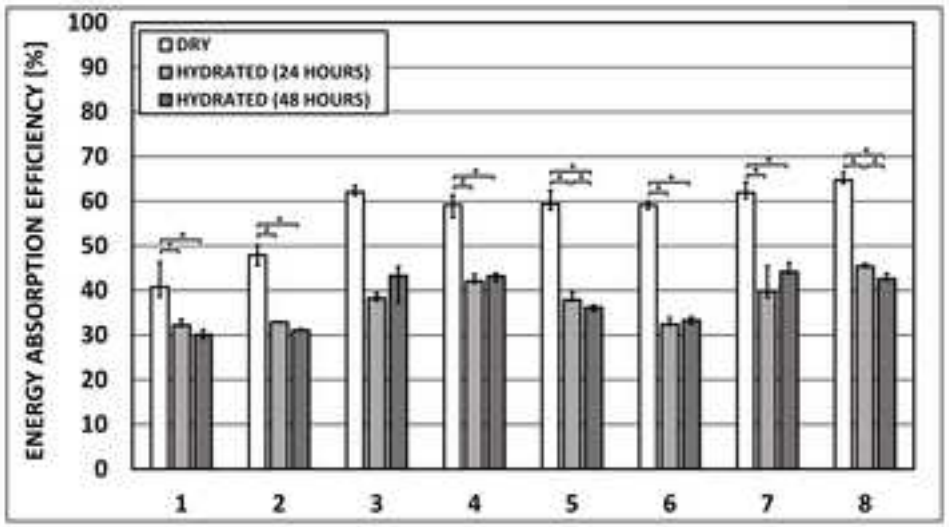

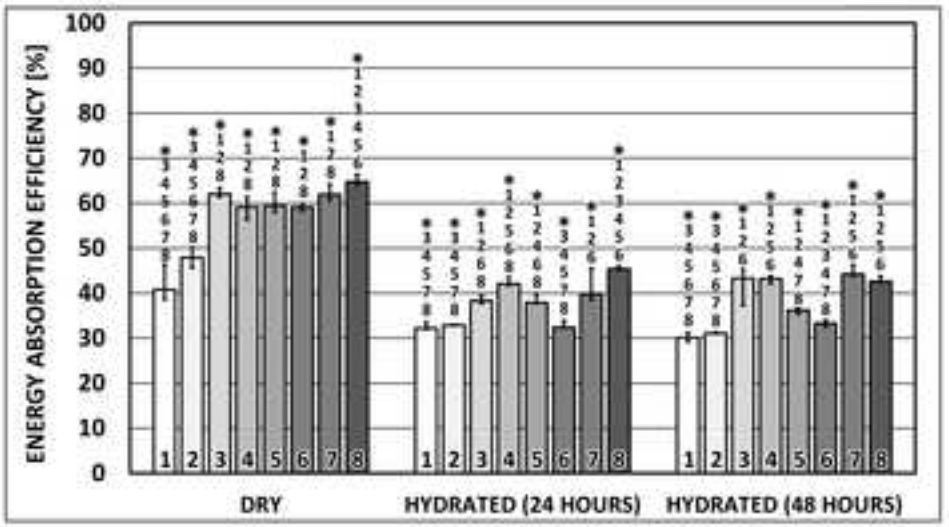

Figure 7

Click here to download Figure FIGURE_7.tif

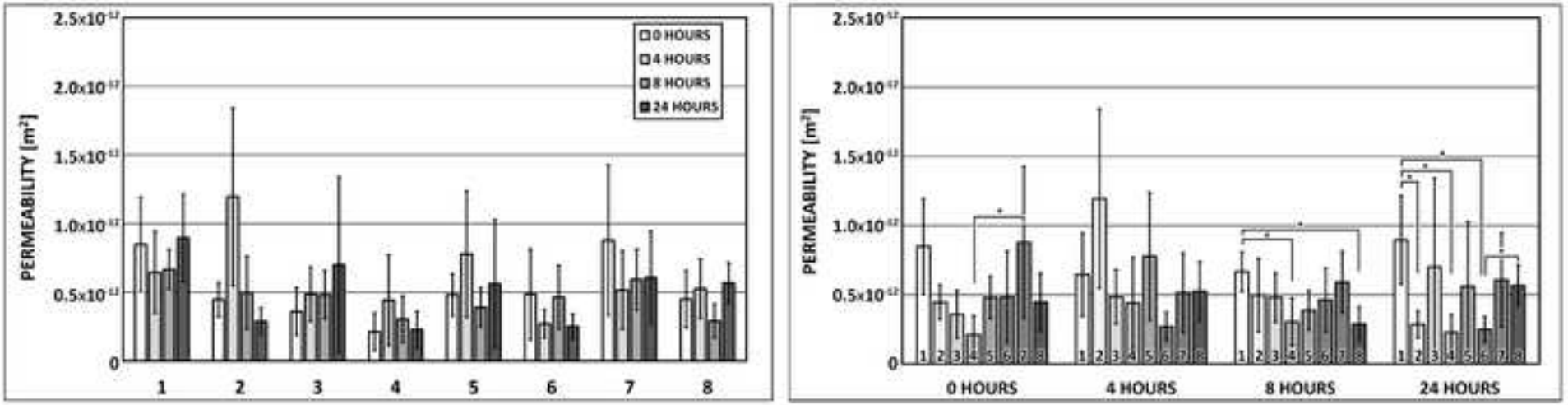

Figure 8

Click here to download Figure FIGURE_8.tif

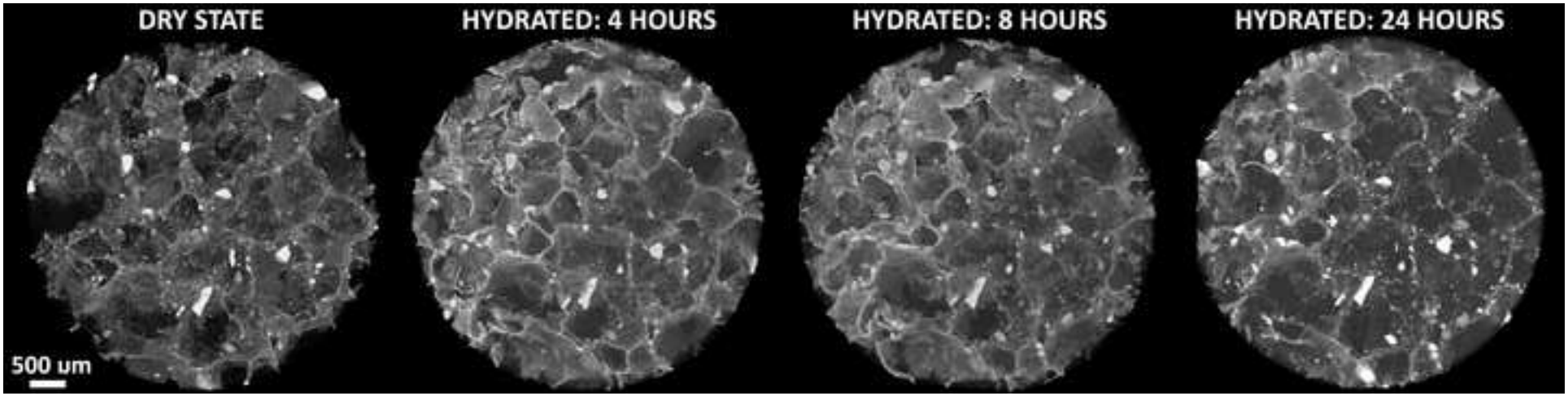

Figure 9

Click here to download Figure FIGURE_9.tif

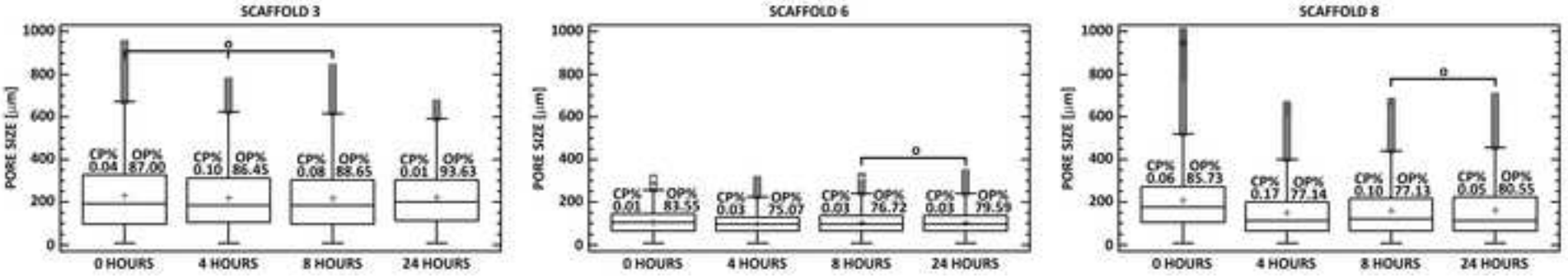

Figure 10

Click here to download Figure FIGURE_10.tif

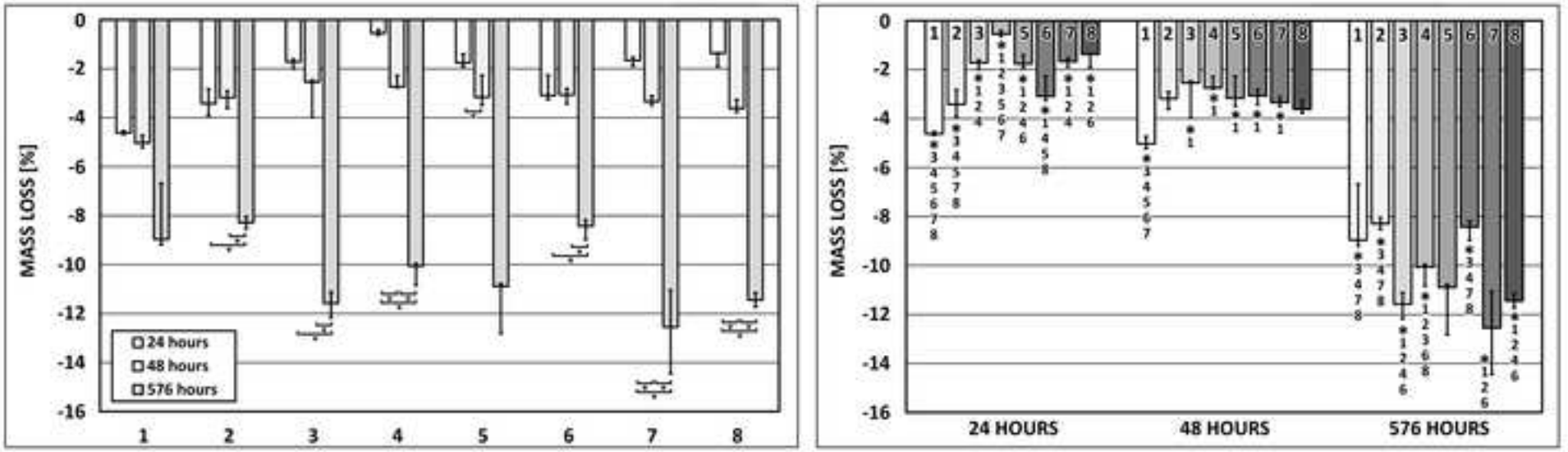

Figure 11

Click here to download Figure FIGURE_11.tif

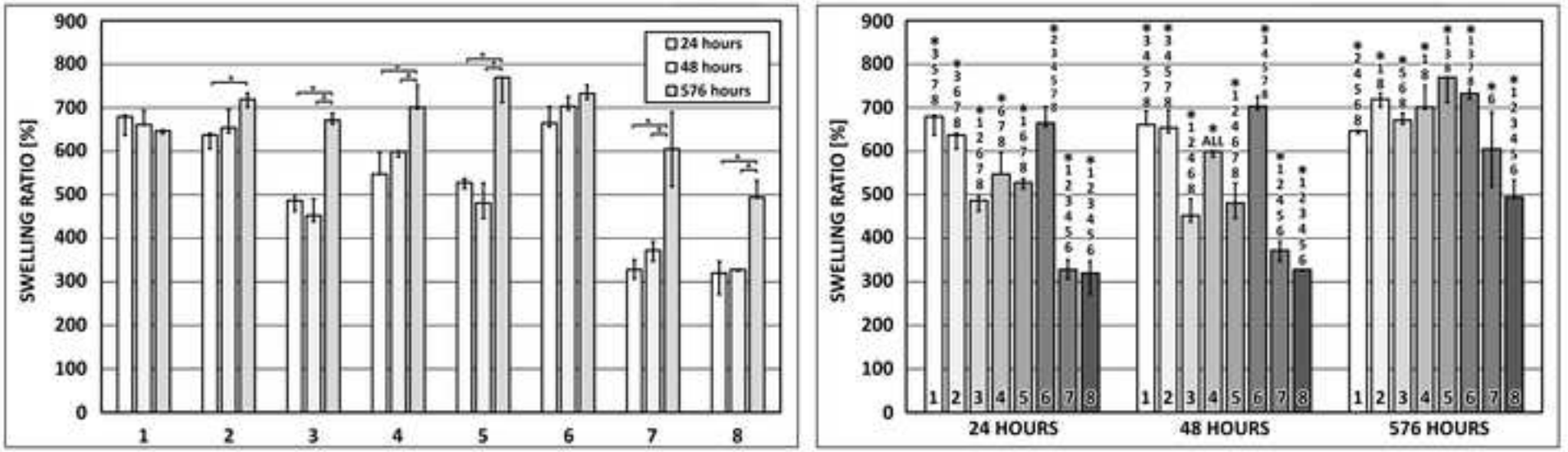

Figure 12

Click here to download Figure FIGURE_12.tif

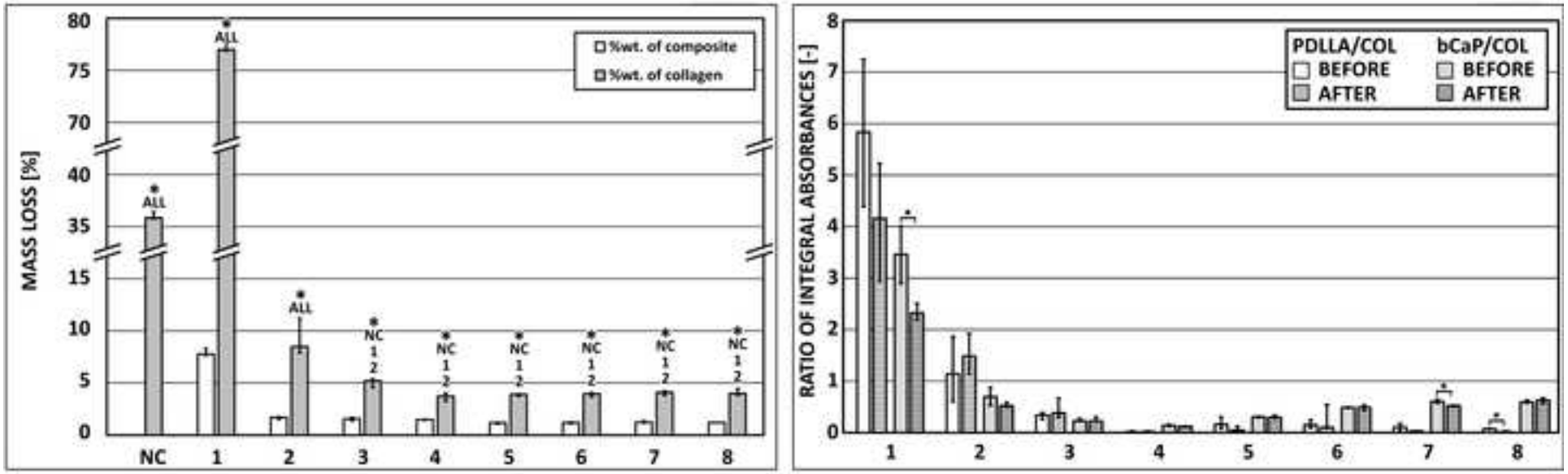

Supplementary figure

Click here to download Figure SUPPLEMENT_1.tif

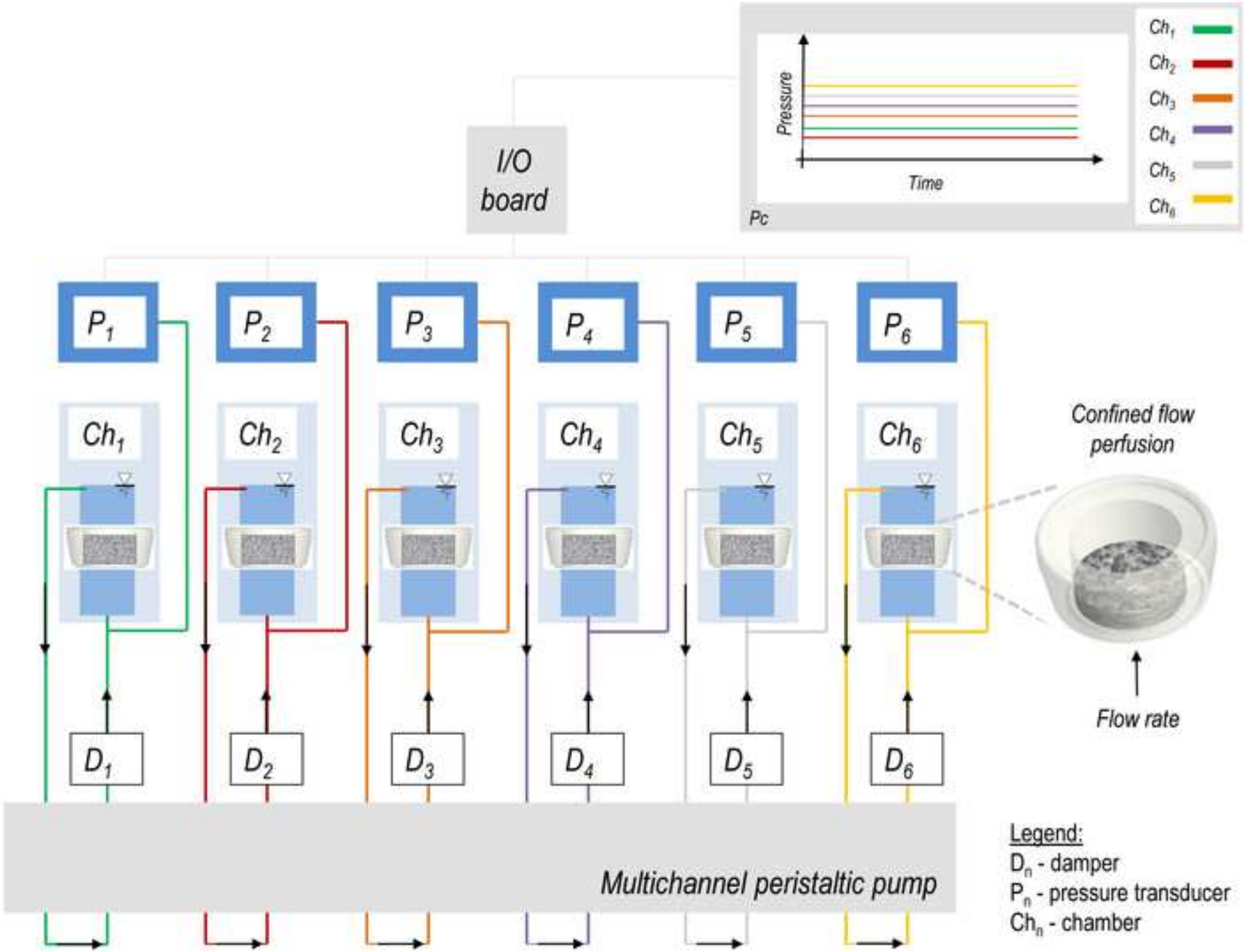

Graphical Abstract